Unconventional Temperature Enhanced Magnetism in Fe_{1.1}Te

Igor A. Zaliznyak, Zhijun Xu, John M. Tranquada, Genda Gu, Alexei M. Tsvelik, and Matthew B. Stone

Unconventional temperature enhanced magnetism in $\mathrm{Fe}_{1.1}\mathrm{Te}$.

Igor A. Zaliznyak,[1, *] Zhijun Xu,[1] John M. Tranquada,[1] Genda Gu,[1] Alexei M. Tsvelik,[1] and Matthew B. Stone[2]

[1]*CMPMSD, Brookhaven National Laboratory, Upton, NY 11973 USA*
[2]*Oak Ridge National Laboratory, 1, Bethel Valley Road, Oak Ridge, Tennessee 37831, USA*

Our inelastic neutron scattering (INS) study of spin excitations in iron telluride reveals remarkable thermal evolution of the collective magnetism. In the temperature range relevant for the superconductivity in $\mathrm{FeTe}_{1-x}\mathrm{Se}_x$ materials, where the local-moment behavior is dominated by liquid-like correlations of emergent spin plaquettes, we observe unusual, marked increase of magnetic fluctuations upon heating. The effective spin per Fe at T $\approx$ 10 K, in the phase with weak antiferromagnetic order, corresponds to S $\approx$ 1, consistent with the recent analyses that emphasize importance of Hund's coupling [1]. However, it grows to S $\approx$ 3/2 in the high-T disordered phase, suggestive of the Kondo-type behavior, where local magnetic moments are entangled with the itinerant electrons.

Magnetic fluctuations discovered by INS [2–4], are believed to be of vital importance for both copper- and iron-based high-temperature superconductors (HTSC) [5–7]. In two competing scenarios, they either originate from local atomic spins [8], or are a property of cooperative spin-density-wave (SDW) behavior of conduction electrons [9, 10]. Here, we report an INS study of spin dynamics in iron telluride, a parent material of the simplest family of iron-based HTSC, aimed at resolving this issue.

Iron telluride becomes superconducting upon partial, or full isoelectronic substitution of Te by Se [11, 12]. Although the highest critical temperature for $\mathrm{FeTe}_{1-x}\mathrm{Se}_x$ is only $T_c \approx 14.5$ K, it increases to above 30 K under pressure [13]. FeTe crystal structure consists of a continuous stacking of square-lattice layers of iron atoms, each sandwiched between the two twice-sparser layers of bonding chalcogen/pnictogen atoms, which is the basic structural motif for all iron-based superconductors. The Te atoms, which tetrahedrally coordinate the Fe sites, occupy alternate checkerboard positions above and below the Fe layer, so that the resulting unit cell contains two formula units. In this quasi-two-dimensional structure, FeTe layers are are only weakly bound together and crystallographic stability is improved if some amount of extra Fe atoms is incorporated between the layers, which frustrates magnetic correlations in the $\mathrm{Fe}_{1+y}\mathrm{Te}$ series $(0.02 < y < 0.11)$. As we discuss later, this has important consequences for magnetic order and lattice distortion, which in our $\mathrm{Fe}_{1.1}\mathrm{Te}$ sample are noticeably weaker than in samples with $y \lesssim 0.06$ [14–16], and for low-energy magnetic correlations, which are more diffuse.

Band structure calculations predict Fe(Te,Se) to be a metal, with several bands crossing the Fermi energy [17–19]. This qualitatively agrees with scanning tunneling spectroscopy [20] and angle-resolved photoemission studies of FeTe [21, 22]. Both find small electron and hole pockets near the corner, $\boldsymbol{Q} = (0.5, 0.5)$, and the center, $\boldsymbol{Q} = 0$, respectively, of the two-dimensional (2D) Brillouin zone (BZ) (we use reciprocal lattice units (r. l. u.) notations corresponding to the actual crystallo-

graphic unit cell with 2 Fe atoms). While these findings reveal the existence of itinerant electrons, bulk resistivity measurements find either a non-metallic, or a bad-metal behaviour. At the same time, Curie-Weiss behaviour of magnetic susceptibility suggests significant local magnetic moments, $\mu_{eff} \approx 4\mu_B$ (μ_B is Bohr's magneton), and a rather small Curie-Weiss temperature, $\Theta_{CW} \approx 190$ K [14, 23, 24]. Thus, we have materials where local moments and itinerant conduction electrons coexist, and the relation between them is revealed by our experiments.

Our measurements were carried out using the ARCS spectrometer at the Spallation Neutron Source at Oak Ridge National Laboratory. The $\mathrm{Fe}_{1.1}\mathrm{Te}$ crystal of $m = 18.45$ g with a mosaic of $2.2°$ full width at half maximum (FWHM) was mounted on an aluminium holder attached to the cold head of closed-cycle refrigerator. The crystal's c-axis was aligned parallel to the incident neutron beam, with the a-axis at about $24°$ to the horizontal. ARCS is a direct geometry, time-of-flight spectrometer, where a monochromatic pulse of neutrons with energy E_i is incident on the sample. For each energy transfer, $E < E_i$, a slice of the sample's $\boldsymbol{Q} = (h, k, l)$ phase space is probed. We analyzed projections of such slices on the (h, k)-plane. Each (h, k) point corresponds to a particular value of $l = l(h, k, E, E_i)$, since $\boldsymbol{Q}$ and E are coupled via energy-momentum conservation. For $E_i = 40$ meV, magnetic Bragg peaks arising from the three-dimensional (3D) magnetic ordering at wave vector $\approx (0.5, 0, 0.5)$ can be observed in the second Brillouin zone, Fig. 1(a), because $l(0.5, 1, 0, 40) \approx 0.5$. $\boldsymbol{Q}-$ and $T-$independent background (BG) arising from the incoherent elastic scattering was estimated at several positions where magnetic scattering is nearly absent, and subtracted from all data. It had the form of the resolution-limited (FWHM = 2 meV) Gaussian peak in energy. Data was normalized to the inelastic scattering intensity from acoustic phonon modes near the structural Bragg reflection $\boldsymbol{\tau} = (1, 1, 1)$.

Figure 1 presents an overview of the low-energy magnetic excitations at T = 10 K. The left column shows neutron intensity as a function of the 2D wave vector
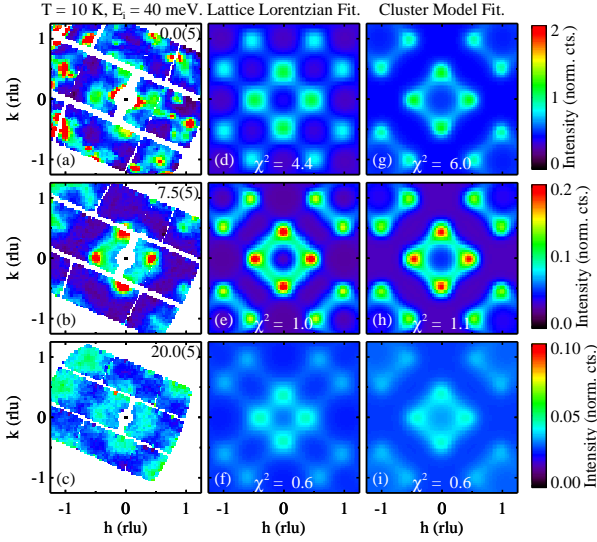
Figure 1: Magnetic scattering intensity measured in $Fe_{1.1}Te$ at T = 10 K for energy transfers (0 ± 0.5) meV, (a), (7.5 ± 0.5) meV, (b) and (20 ± 0.5) meV, (c). (d)-(f), fits to a model cross section consisting of four lattice Lorentzian (LL) peaks at $(0,\pm\zeta)$ and $(\pm\zeta,0)$, $\zeta \lesssim 0.5$. A Gaussian ring of scattering centered at $(0,0)$ is included in (e) to account for the dispersive acoustic mode clearly visible in Fig. 2(a). (g)-(i), two-parameter fits to the checkerboard cluster model described in the text. All fits assume the magnetic form factor of Fe^{2+}.

Figure 2: Energy dependence of the imaginary part of the dynamical magnetic susceptibility, $\chi''(\boldsymbol{Q},E) = \pi(1 - e^{-E/(k_BT)})S(\boldsymbol{Q},E)$ at T = 10 K, (a), 80 K, (d), and 300 K, (g), as a function of wave vector $(0,K)$. (b), (e), (h) and (c), (f), (i) show fits to the same models as in Fig. 1.

$\boldsymbol{Q} = (h,k)$ in the ab-plane for elastic, $E = 0$, (a), and inelastic, $E = 7.5$ meV, (b), and 20 meV, (c), scattering. Remarkably, the scattering takes the form of broad, diffuse peaks centered near (but not exactly at) $(\pm0.5,0)$ and $(0,\pm0.5)$ positions, for all energies covered in this measurement $(E \lesssim 26$ meV). Magnetic dynamics of this type is often explained by invoking a system of itinerant electrons, where wave vectors of magnetic excitations are determined by nesting properties of the Fermi surface(s) [9, 10, 17]. Such explanation clearly fails for FeTe compounds, since there is no Fermi surface nesting near $(0.5,0)$ – nesting occurs at $(0.5,0.5)$ and $(1,0)$ [20]. In addition, as we show later, the large observed magnetic intensity would require the entire weight of two fully spin-polarized itinerant electronic bands.

The magnetic excitations in Fig. 1 imply robust short-range correlations, whose well-defined real space structure persists over a broad range of time scales. In a system of local spins this might be a signature of an emergent cooperative spin texture, such as the hexagonal loops induced by spin frustration in $ZnCr_2O_4$ [25, 26]. While our attempts to analyze the low-energy magnetic scattering in $Fe_{1.1}Te$ in terms of spin waves in the Heisenberg model were unsatisfactory, we found that the observed scattering can be very accurately described by a cluster model of this kind. The right column of Fig. 1 shows fits of our data to a model in which plaquettes of four ferromagnetically co-aligned nearest-neighbor Fe spins emerge as a new collective degree of freedom, with short-range antiferromagnetic correlations between
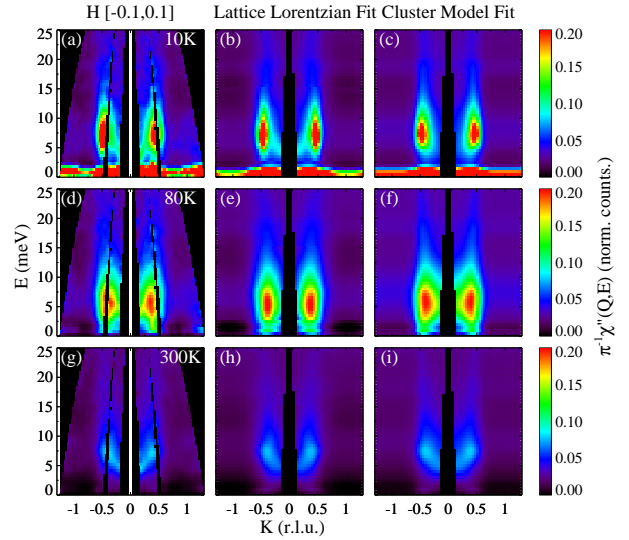
the neighboring plaquettes. Such co-aligned plaquettes are locally favored by Fe interstitials, a small amount of which is present in our sample and which act as condensation centers for plaquette spin liquid. The absence of magnetic scattering along the sides of the square with vertices at $(h,k) = (\pm1,0),(0,\pm1)$ is a clear fingerprint of the plaquette structure factor, $S_p(\boldsymbol{Q}) \sim |\cos(\pi(h+k)/2)\cos(\pi(h-k)/2)|^2$. With only two parameters, the intensity and the correlation length ξ, this fit is nearly as good as the fit to the phenomenological pattern of factorized Lorentzian peaks shown in Fig. 1 (d)-(f), which was used for quantifying intensity and position of magnetic scattering in Figures 2 and 3.

Figure 2 shows the energy dependence of magnetic intensity at $h \approx 0$, corresponding to the vertical slice at the center of Fig. 1 (a)-(c). It reveals a pronounced maximum at $E \approx 7$ meV and a weak, acoustic-like mode dispersing from it down to $Q = 0$. While the origin of the resonance-like maximum is unclear, it appears near the same energy as the spin resonance at (π,π) in superconducting $FeTe_{1-x}Se_x$ samples [4]. Our supplementary measurements have revealed that magnetic scattering pattern in $Fe_{1.1}Te$ begins changing noticeably above ~ 30 meV, and at high energies has similar shape to that in $FeTe_{1-x}Se_x$ [4]. We find that magnetic fluctuations in $Fe_{1.1}Te$ extend to ≈ 190 meV, an order of magnitude larger energy than $k_B\Theta_{CW}$. This is a clear signature of competing interactions. Indeed, the former scale pertains to the energy associated with a flip of a single spin thus giving a typical value of the exchange coupling, while Θ_{CW} is determined by the sum of all exchange couplings. Its relative smallness in $Fe_{1+y}Te$ indicates an almost complete cancelation of the dominant next-nearest neighbor Fe-Te-Fe antiferromagnetic superexchange and the ferro-
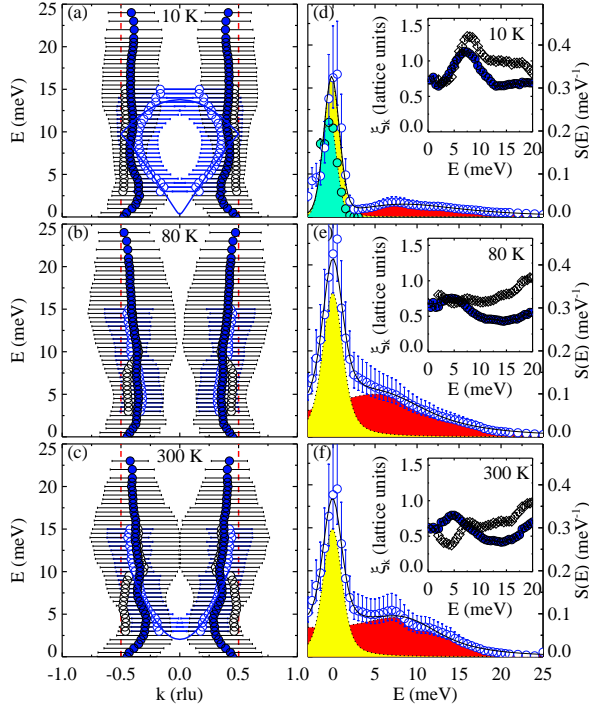
Figure 3: Peak positions at T = 10 K, (a), 80 K, (b), and 300 K, (c), obtained by fitting constant-E slices to a single-component LL cross-section (filled symbols). Horizontal bars show the FWHM of LL peaks. Open symbols are positions of the LL (black) and the ring (light blue with error bars) in the two-component model of Fig. 2 (e). Solid line in (a) is a fit of the ring mode dispersion to $E(q) \sim \sin(\pi k/2)$, folded into a small (magnetic) Brillouin zone, $[-0.5, 0.5]$. (d), (e), (f) Integral intensity of magnetic scattering as a function of energy. Error bars account for the uncertainty of absolute normalization. Solid lines are fits consisting of a quasi-elastic (QE) central peak (shaded yellow) and a damped harmonic oscillator (DHO, red), used to interpolate the data for integration. Green-shaded peak in (d) is magnetic Bragg intensity. Insets show the correlation length in lattice units for the LL (closed circles) and the cluster (open rhombi) models.

magnetic coupling between the nearest neighbors, which is probably mediated by itinerant electrons.

As far as the low energy magnetic fluctuations are concerned, it is tempting to pursue further the analogy with emergent excitations of frustrated spins in $ZnCr_2O_4$. There, a somewhat similar resonance behavior was observed. It arises upon cooling, as a result of interaction with the lattice, and is accompanied by a small lattice distortion and a weak long-range antiferromagnetic order [25, 26]. $Fe_{1+y}Te$ materials also exhibit antiferromagnetic order, which is coincident with small monoclinic distortion of the crystal lattice [14, 15]. At high T both systems have similar effective Curie-Weiss fluctuating moment of $\sim 4\mu_B$, and in both cases only a fraction of the moment participates in the long-range antiferromagnetism.

Magnetic order in our $Fe_{1.1}Te$ sample occurs at $T_N \approx$ 58 K, about 10 K lower than at lower y, and without sharp discontinuities in T-dependencies, consistent with

the idea that interstitial Fe induces magnetic frustration. Analysis of magnetic Bragg intensities visible in the 10 K data of Fig. 1(a) near $(\pm 1, \pm 0.5)$, yields long range ordered moment of $\approx 1\mu_B$, about twice smaller than for $y \approx 0.05$ [14, 15]. However, there is also a significant amount of elastic or nearly elastic 2D magnetic diffuse scattering near $(0, \pm 0.5)$, $(\pm 0.5, 0)$ in our sample, which results from frozen, or very slowly fluctuating short-range correlations. The total spectral weight of magnetic Bragg and diffuse scattering adds to $\approx 2.3\mu_B$, which is similar to the ordered moment in lower-y samples.

Recall, that for a system of spins S, magnetic neutron scattering intensity is determined by the product of magnetic form factor, which accounts for the electronic magnetization density associated with each spin, and the dynamical correlation function $S(\boldsymbol{Q}, E)$, which describes cooperative motions of spins. The total spectral weight of $S(\boldsymbol{Q}, E)$ obeys the sum rule, $\int S(\boldsymbol{Q}, E)d^3\boldsymbol{Q}dE = S(S + 1) = [\mu_{eff}/(g\mu_B)]^2$, where we omit polarization indices and imply trace over spin polarizations; g is the Lande factor. This defines the fluctuating instantaneous effective moment, μ_{eff}, whereas the ordered static moment is $g\mu_B\langle S\rangle$, where $\langle S\rangle$ is the ground-state value of spin-S operator, with $g\mu_B\langle S\rangle < g\mu_B S < \mu_{eff}$. Figure 3a shows that magnetic Bragg peaks account for only $\approx 28\%$ of the total intensity, while another $\approx 28\%$ are in the inelastic spectrum. By energy-integrating all contributions, we obtain $\mu_{eff} = 2.7(7)\mu_B$ at 10 K, which is very close to $\approx 2.8\mu_B$ expected for $S = 1$ and $g = 2$.

Thus, only about a half of the total magnetic intensity expected for $\mu_{eff} \approx 4\mu_B$, which is obtained from the uniform CW susceptibility, is accounted in our T = 10 K data. This already suggests that we do not deal with just a system of local spins. The temperature dependence provides further striking evidence. Indeed, for a system of spins S, the sum rule requires that the integral of $S(Q, E)$ remains constant $(= S(S + 1))$ at all temperatures. The magnetic scattering in the insulating $ZnCr_2O_4$ is consistent with local moments that do not change with temperature. In $Fe_{1.1}Te$ the behavior is markedly different, which is already clear from Figs. 2 and 3. We find that total magnetic INS intensity significantly increases upon heating, as summarized in Fig. 4(c). The total magnetic spectral weight at 300 K yields $\mu_{eff} \approx 3.6\mu_B$, close to the value of $\approx 3.9\mu_B$ corresponding to S = 3/2 and in good agreement with the susceptibility data. Thus, the overall picture is of a temperature-induced change from local spins S = 1 at 10 K to S = 3/2 at 300 K. This can only occur as a result of an effective change by 1 of the number of localized electrons, with a corresponding change in the number of itinerant electrons.

Having made this surprising discovery, we performed a more detailed survey of the temperature dependence of $S(Q, E)$. Figure 4(b) shows the resulting wave-vector-integrated correlation function, $S(E)$, on a logarithmic scale, which emphasizes the changing balance between
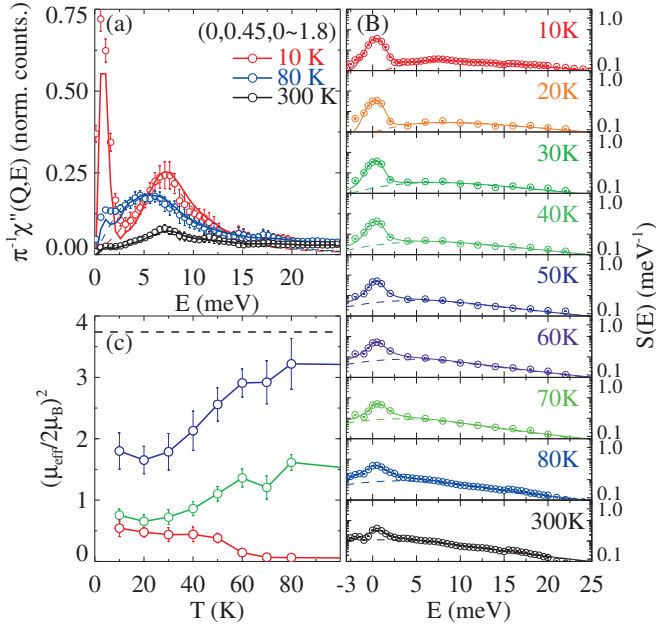
Figure 4: (a) $\chi''(\boldsymbol{Q}, E)$ as a function of energy for $\boldsymbol{Q} = (0, 0.45)$ at 10 K, 80 K and 300 K. Lines are fits shown in Fig. 2(b),(e),(h). (b) Temperature dependence of $S(E)$, excluding Bragg scattering. Solid lines are fits of Fig. 3(d)-(f), dashed lines show DHO fits of the inelastic part. (c) Square of the effective magnetic moment obtained by integrating the $S(E)$, as a function of temperature. Upper (blue) symbols show the total response, bottom (red) symbols are the Bragg contribution, green symbols are the quasi-elastic contribution.

and their interaction with itinerant electrons in a manner conductive for the superconductivity. To our knowledge, the temperature-induced enhancement of local magnetic moments that we have found in iron telluride has never before been observed in a magnetic iron group material. After this paper was completed, data on $Fe_{1+y}Te$ with different y appeared, showing traces of this behavior [16]. This effect calls for conceptually new approaches to understanding HTSC, as it has not been anticipated by any theoretical work, and is not expected in a description based on rigid bands for the conduction electrons.

quasi-elastic and inelastic fluctuations. As illustrated in Fig. 4(a), the resonance character of the inelastic spectrum in $Fe_{1.1}Te$ is clearly retained even at 300 K, in contrast to the behavior of frustrated local spins in the insulating $ZnCr_2O_4$. It is this resonance mode which is the main beneficiary of the additional temperature-induced spectral weight in $S(E)$. A possible origin of such a diffuse resonant mode is screening of the local moments by the conduction electrons, as in the Kondo effect.

Finally, the sum of the temperature-dependent magnetic Bragg intensity and the quasi-elastic 2D diffuse scattering in Fig. 4(c) is nearly T-independent right through T_N and beyond. This suggests that both long-range antiferromagnetism, and the monoclinic distortion, likely are only modest perturbations to the emergent spin dynamics, which is governed by much stronger interactions of local spins and itinerant electrons.

While the relevance of magnetic correlations to HTSC is widely acknowledged, the nature of the magnetism has been controversial [5–10]. Here, for a system bearing an immediate relation to HTSC, we have presented direct experimental evidence for emergent local spin magnetism non-trivially coupled to the itinerant electrons. While the nature of the local spin clusters which govern low-energy magnetic fluctuations in $Fe_{1.1}Te$ is clearly not favorable for the HTSC, perhaps a slight change of the electronic structure in $FeTe_{1-x}Se_x$ modifies the emergent modes

* Electronic address: zaliznyak@bnl.gov

[1] K. Haule, G. Kotliar, New J. Phys. **11** 025021 (2009).

[2] R. J. Birgeneau, C. Stock, J. M. Tranquada, and K. Yamada, J. Phys. Soc. Jpn. **75**, 111003 (2006).

[3] J. W. Lynn, P. C. Dai, Physica C **469**, 469 (2009).

[4] M. D. Lumsden, A. D. Christianson, J. Phys. Condens. Matter **22**, 203203 (2010).

[5] D. J. Scalapino, Physica C **470**, S1 (2010).

[6] P. Monthoux, D. Pines, G. G. Lonzarich, Nature **450**, 1177 (2007).

[7] I. I. Mazin, D. J. Singh, M. D. Johannes, M. H. Du, Phys. Rev. Lett. **101**, 057003 (2008).

[8] Q. Si, E. Abrahams, J. H. Dai, J.-X. Zhu, New J. Phys. **11**, 045001 (2009).

[9] A. V. Chubukov, D. V. Efremov, I. Eremin, Phys. Rev. B **78**, 134512 (2008).

[10] V. Cvetkovic, Z. Tesanovic, Europhys. Lett. **85**, 37002 (2009).

[11] K.-W. Yeh, *et al.*, Europhys. Lett. **84**, 37002 (2008).

[12] F.-C. Hsu, *et al.*, Proc. Natl. Acad. Sci. U.S.A. **105**, 14262 (2008).

[13] S. Margadonna, *et al.*, Phys. Rev. B **80**, 064506 (2009).

[14] T. J. Liu, *et al.*, Nature Materials **9**, 717 (2010).

[15] A. Martinelli, *et al.*, Phys. Rev. B **81**, 094115 (2010).

[16] C. Stock, *et al.*, Phys. Rev. B **84**, 045124 (2011).

[17] I. I. Mazin, Nature **464**, 183 (2010).

[18] A. Subedi, L. Zhang, D. J. Singh, M. H. Du, Phys. Rev. B **78**, 134514 (2008).

[19] Fengjie Ma, Wei Ji, Jiangping Hu, Zhong-Yi Lu, Tao Xiang, Phys. Rev. Lett. **102**, 177003 (2009).

[20] T. Hanaguri, S. Niitaka, K. Kuroki, H. Takagi, Science **328**, 474 (2010).

[21] Y. Xia, *et al.*, Phys. Rev. Lett. **103**, 037002 (2009).

[22] Y. Zhang, *et al.*, Phys. Rev. B **82**, 165113 (2010).

[23] G. F. Chen, *et al.*, Phys. Rev. B **79**, 140509(R) (2009).

[24] Rongwei Hu, E. S. Bozin, J. B. Warren, C. Petrovic, Phys. Rev. B **80**, 214514 (2009).

[25] S.-H. Lee, *et al.*, Nature **418**, 856 (2002).

[26] S.-H. Lee, C. Broholm, T. H. Kim, W. Ratcliff, S.-W. Cheong, Phys. Rev. Lett. **84**, 3718 (2000).